JOURNAL OF Applied Polymer SCIENCE

Synthesis and Characterization of Microencapsulated Sodium Phosphate Dodecahydrate

Ting Yu Wang, Jin Huang
School of Materials and Energy, Guangdong University of Technology, 510006 Guangzhou, People's Republic of China
Correspondence to: J. Huang (E-mail: huangjiner@126.com)

ABSTRACT: Microcapsules loaded with sodium phosphate dodecahydrate (DSP) were prepared according to the solvent evaporation method. The microencapsulated phase-change materials (MEPCMs) possessed methyl methacrylate crosslinked with ethyl acrylate generated poly(methyl methacrylate) (PMMA) as the coating polymer. The influences of the polymerization time, polymerization temperature, and organic solvent types on the performances of the MEPCMs were studied in this report. The results indicate that the polymerization time and temperature had barely any effect on the size but a significant effect on the surface morphology of the microphase-change materials. The solubility of the shell material varied in different organic solvents, and this to different phase-transition enthalpies. In addition, DSP could be encapsulated well by PMMA, and the as-prepared MEPCMs were equipped with a good morphology and a small particle size. When toluene and acetone were used as organic solvents, the MEPCMs had an interesting energy storage capacity of 142.9 J/g at 51.51°C, and this made them suitable for different applications. © 2013 Wiley Periodicals, Inc. J. Appl. Polym. Sci. 130: 1516–1523, 2013

KEYWORDS: copolymers; differential scanning calorimetry (DSC); inorganic polymers; thermal properties

Received 14 November 2012; accepted 28 February 2013; Published online 30 April 2013
DOI: 10.1002/app.39249

INTRODUCTION

Latent heat-storage technology has aroused considerable scientific concern because it can gain a high energy storage density, large heat-storage capacity, and heat energy release at a constant temperature or over a small temperature range, corresponding to the phase-transition temperature of the phase-change materials (PCMs).[1–7] Solid–liquid PCMs are often used for solar heat-storage applications, building energy savings, battery thermal management, and so on.[8–10] Although more than thousands of PCMs are available in nature, only a small amount of them are suitable for practical applications, and no single material can contain all desirable properties. For the sake of overcoming the problems of conventional PCMs, including corrosion on metals, decomposition, supercooling, and leakage, encapsulated PCMs have received growing attention for thermal energy storage in recent years.[11–15] The production of polymeric nonspherical particles and particles with special morphologies at 1–5 μm has received a great deal of attention over the years.[16]

However, the research and development work of textiles containing PCMs have essentially focused on organic compounds. The use of salt hydrates and their supercooling properties are exploited for specialized thermal storage applications. A few inorganic microencapsulated phase-change material (MEPCMs) have been prepared by the solvent evaporation method. For example, Zhang et al.[17] proposed the encapsulation of $Na_2SO_4{\cdot}10H_2O$–SiO_2 with an *in situ* polymerization method, which improved the supercooling and segregation of $Na_2SO_4{\cdot}10H_2O$.[17] Salaün et al.[18] discussed the influence of different solvents on the morphology of microcapsules and obtained a coating rate of 68.4% and a uniform distribution of sodium phosphate dodecahydrate (DSP)–polyurethane microcapsules when toluene and chloroform were used as organic solvents.

Meanwhile, the microencapsulation of PCMs involves enclosing them in thin and resilient polymer shells so that the PCMs can be changed from solid to liquid and back again within the shells.[19–21] In numerous applications, MEPCMs are required to provide good thermal characteristics and mechanical strength to ensure an intact structure during the manufacturing processes.[22–24] Therefore, core materials need to be encapsulated in a thin and flexible polymer shell, and the PCMs in it could change from solid into liquid state and then restore.[25] To reduce the brittleness of poly(methyl methacrylate) (PMMA) and improve the processing performance, 5–20% ethyl acrylate (EA) used as a second monomer is often added to carry out the polymerization.

In this study, the MEPCMs possessed DSP as a core material and modified PMMA copolymer as a shell material. The surface

morphology was investigated by phase-contrast microscopy and scanning electron microscopy (SEM) on a mesoscopic scale. Transmission electron microscopy (TEM) was used to investigate the composition and morphology on a microscopic scale. Moreover, the analysis of the thermal properties was investigated by differential scanning calorimetry (DSC). Through the previous analysis, we found that the functional performances of the as-prepared MEPCMs were influenced by the process parameters, including the polymerization time, polymerization temperature, and type of organic solvent.

EXPERIMENTAL

Materials

DSP ($Na_2HPO_4 \cdot 12H_2O$) was used as a core material. Methyl methacrylate (MMA) and EA were used as monomers. The nonionic surfactant sorbitan trioleate (Span85) was used as an emulsifier. Benzoyl peroxide (BPO; 97 wt %) was used as a radical initiator. Toluene, carbon tetrachloride, chloroform, and acetone of reagent grade were used as organic solvents. The previous reagents were reagent grade and purchased from Tianjin Damao Co., Ltd.

Preparation

The theory of microcapsulation by the solvent evaporation method was described previously elsewhere.[18] In this study, the preparation of the DSP–PMMA MEPCMs was carried out according to the following steps. In a typical procedure, DSP (22.5, 15, and 10 g for D1, D2, and D3, respectively) was melted into a liquid and then mixed with 50 mL of organic solvent A (carbon tetrachloride or toluene). This was followed with the emulsification by an ultrasonic mill (800w) for 15 min (Xinzhi JY92-2D, Ningbo, China). Next, 5 g of deionized water as additional supplementary water was added. When the expected droplet size of the emulsion was reached, a solution containing 12.5 mL of MMA previously dissolved in 30 mL of volatile organic solvent B (acetone, carbon tetrachloride, or chloroform) was added. After the mixture (900 rpm) was stirred for 30 min at 80°C, precipitation was initiated by the dripping of an EA solution (2.5 mL of EA dissolved in 10 mL of organic solvent A) and additives of BPO. The reaction mixture was kept at 80–90°C for 4 h in a three-outlet flask. Ultimately, the resulting microcapsules (D1, D2, and D3, respectively) were purified by centrifugation three times to remove the residual reagents and dried at 60°C for 24 h.

Characterization

The morphology of the DSP–PMMA MEPCMs were observed by phase-contrast microscopy (Japan, OLYMPUS, CX41) equipped with a camera (Japan, Nikon, COOLPIX4500).

The morphology and dispersion state of the microcapsules were observed with the help of SEM (Hitachi, S-3400N, Japan). The samples were treated by gold spraying before the test.

The deeply compositional and morphological analysis was observed by TEM (JEOL, JEM-3010, Japan).

The spectroscopic analyses of the microcapsules were performed with a Fourier transform infrared (FTIR) instrument (American, Thermo Fisher Scientific, Nicolet 6700) on a KBr disk.

The thermal behavior of the MEPCMs, including the melting temperature (T_m) and latent heats, were measured with DSC (TA Instruments, DSCQ10). The MEPCM samples were dried to a constant weight before the test. The transition temperatures and enthalpies were obtained at a scanning speed of 5 K/min.

RESULTS AND DISCUSSION

Morphological Analysis of the MEPCMs

MEPCMs are microcontainers made of natural or synthetic polymer materials. The shape and structure of the microcapsules varies with the different properties of the core materials and the preparation method of the microcapsule products. For example, when the structure of a core material is divided into several parts and embedded in the continuous shell material, it changes to a floc state or module form, including multicore or multicore amorphous clusters of microcapsules, and so the situation (Song et al.[26]) is in accordance with our study. Different precision testing means were adopted to observe the morphology of the as-prepared microcapsules, and the phenomenon could be explained as follows.

The phase-contrast microscopy photograph in Figure 1(a) shows the slurry state of the microcapsules. Most of them were obtained with a spherical profile with a smooth and relatively homogeneous external appearance without broken or incomplete parts; they reached the uniform diameter of 2 μm as well. The SEM image of Figure 1(b) shows the powdered state of the microcapsules. They were approximated spherical with a fairly uniform structure and had a particle size around 8.8 μm. Meanwhile, an interesting finding appeared in the TEM photographs of Figure 1(c). From it, one can see the aggregation state of the microcapsules. This may have been due to the microcapsule clusters, which were more closely combined into a similar spherical structure, and this led to a spherical profile appearance in the mesoscopic-scale view but a separated one in the microscopic view. Furthermore, the dispersed state of the microcapsules monomers is presented in Figure 1(d), and the multicore material was wrapped in a irregular wall material. It seemed to be a multicore amorphous microcapsule cluster state on a nanoscale, whereas it appeared as a spherical profile on a mesoscopic scale. The as-prepared microcapsules appeared as a nonsmooth shell, and the shell of polynuclear forms was mainly due to the volatilization of organic solvents during the preparation process. This was in conformity with the study of Song et al.[26] According to the previous analysis of the apparent morphology of the microcapsules, when the mass ratio of DSP to PMMA was 1.5:1, the average MEPCMs cluster unit reached a particle size of 2 μm, which was observed by a lower accuracy test. On the basis of the previous discussion, the MEPCMs were successfully synthesized by means of a solvent evaporation method with DSP as the core.

Chemical Structural Analysis of the MEPCMs

When the materials were added in proportion under the reaction conditions, MMA and EA in the environment of organic solvents began to generate the modified PMMA as shell materials.

Chemical characterization of the MEPCMs was carried out with FTIR spectroscopy. Generally, the FTIR spectrum of MEPCMs

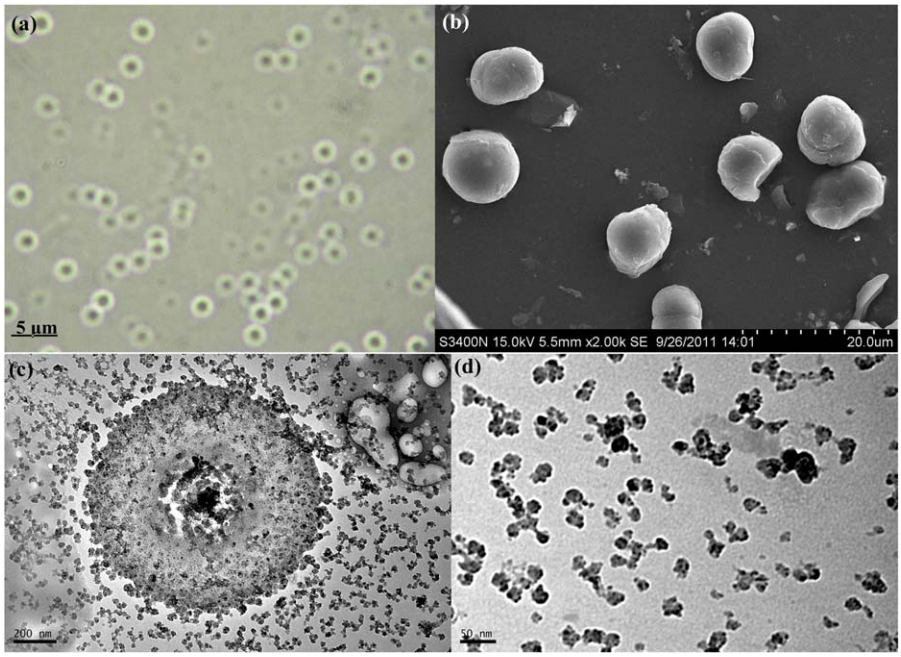

Figure 1. Images of MEPCMs: (a) phase-contrast microscopy image, 1000×; (b) SEM image, 5000×; (c) TEM image, 5×10^4 ×; and (d) TEM image, 2×10^5 ×. [Color figure can be viewed in the online issue, which is available at wileyonlinelibrary.com.]

shows both the characteristic of DSP and PMMA which is shown in Figure 2. The peak around 2950 cm^{-1} was the —CH_2 antisymmetric stretching peak. The peak around 1726 cm^{-1} signified the stretching vibration of the C═O group. The band around 1096 cm^{-1} belonged to the —CH_3 unsymmetrical variable angle vibration. The peak around 989 cm^{-1} was the C—C stretching vibration. Meanwhile, these characteristic peaks, mentioned previously for pure PMMA spectrum, appeared in the corresponding positions of 2925, 1714, 1067, and 995 cm^{-1}, respectively. In addition, in the MEPCM spectrum, the strong peak at 1261 cm^{-1} was the absorption peak of Na_2HPO_4, and the peak at 1137 cm^{-1} was the metaphosphate PO_2 symmetric stretching peak overlapped with the —CH_3 unsymmetrical variable angle vibration peak. Also, it did not appear obviously in the spectrum of PMMA. In line with all of the SEM, TEM, and FTIR spectral observations, it seemed that the microencapsulation of $Na_2HPO_4 \cdot 12H_2O$–PMMA was successfully performed.

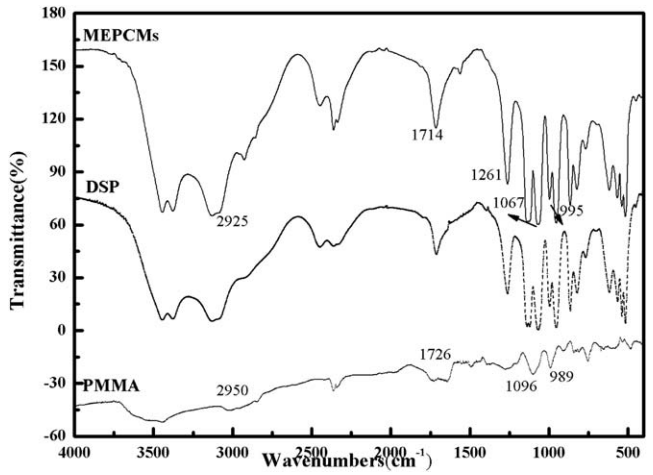

Figure 2. FTIR spectra of the pristine DSP, PMMA, and DSP–PMMA microcapsules.

Thermal Analysis of the MEPCMs

The thermal properties of the resulting MEPCMs, PMMA, and pristine DSP were investigated with DSC (Figure 3). The DSC scan for the pristine DSP sample presented an endothermic peak centered at 34.72°C; this corresponded to the T_m of the pure DSP, and the latent heats of melting (ΔHs) were calculated as 177.8 J/g. To our surprise, for the samples D1, D2, and D3 (with corresponding mass ratios of DSP to PMMA of 1:1.5, 1:1, and 1.5:1), the endothermic peaks were centered at 50.63, 50.74, and 51.51°C, respectively. This meant that T_m increased significantly relative to pristine DSP, whereas their ΔH values decreased to 54.98, 96.25, and 142.90 J/g, respectively. Moreover, there was no such endothermic peak in the DSC scan in the same temperature scope for the pure PMMA curve; this meant PMMA provided no contribution to the phase-change enthalpy of the MEPCMs. From this point of view, the lower phase-change enthalpy of the resulting microcapsules was mainly due to the low filling rate of the DSP to the total MEPCMs, although the T_m increase of the MEPCMs probably originated from the following reasons.

On the one hand, the shift of the phase-transition temperature (T_m) had a close relation to the pore width, which has generally been below 10 nm in the previous reports.[27] This was mainly due to the contribution of the surface free energy; this was associated greatly with the interface between the shell and core materials. With respect to the small pore size, the surface area

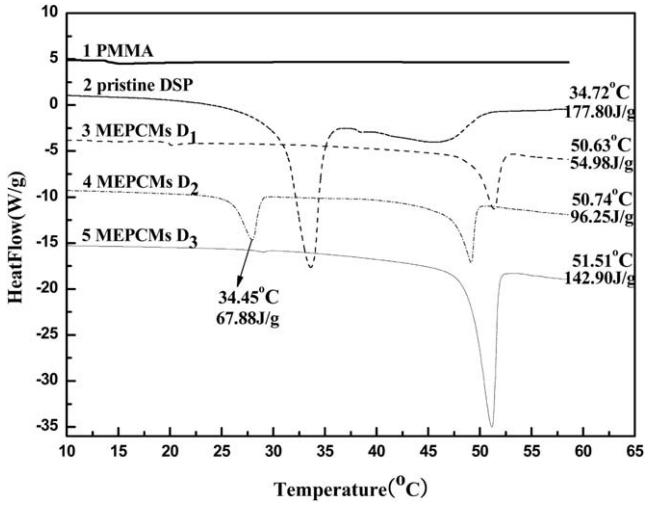

Figure 3. DSC thermograms of the PMMA, DSP, and DSP–PMMA MEPCMs.

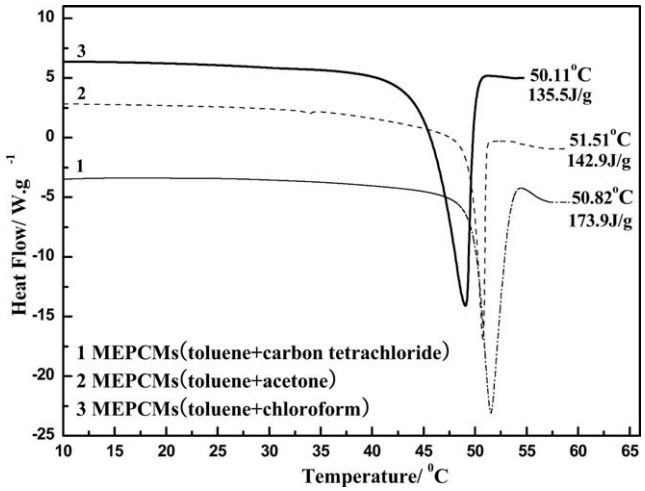

Figure 4. Influence of the organic solvent type on the thermal property of the MEPCMs.

of the core became large compared to its volume, and hence, the contribution of interfacial surface free energy became important in changing the T_m. However, in some recent studies, the T_m's of the MEPCMs were remarkably lower than those of the pristine core material, and the confinement size of their work was obviously larger than tens of nanometers. Herewith, it was found that big difference in the surface tension could also be achieved at large confinement sizes because of the previously mentioned strong interface interactions between the core and shell.[28] A similar situation occurred in our study; the DSC results implied that the T_m's of the MEPCMs were about 17°C higher than those of pristine DSP; this might have originated from the strong interfacial interactions between the core and shell materials of DSP–PMMA MEPCMs. Therefore, the interfacial interaction resulted in a great increase in T_m, despite a confinement size larger than tens of nanometers in the as-prepared MEPCMs.

Another reason for this phenomenon may have been that when AB·mH$_2$O hydrated salt is heated, it usually converts to another type of AB·pH$_2$O.[29] The core material, $Na_2HPO_4 \cdot 12H_2O$, at the prepreprocessing temperature of 25–55°C was perhaps formed of seven hydrated disodium hydrogen phosphates ($Na_2HPO_4 \cdot 7H_2O$), which would be used in the latter preparation procedure in the following as shown in eq. (1). The T_m of $Na_2HPO_4 \cdot 7H_2O$ was about 48°C, [30] and this was close to T_m of the MEPCM D_1, D_2, and D_3, which was about 51°C. This was in agreement with the previous FTIR examinations as well:

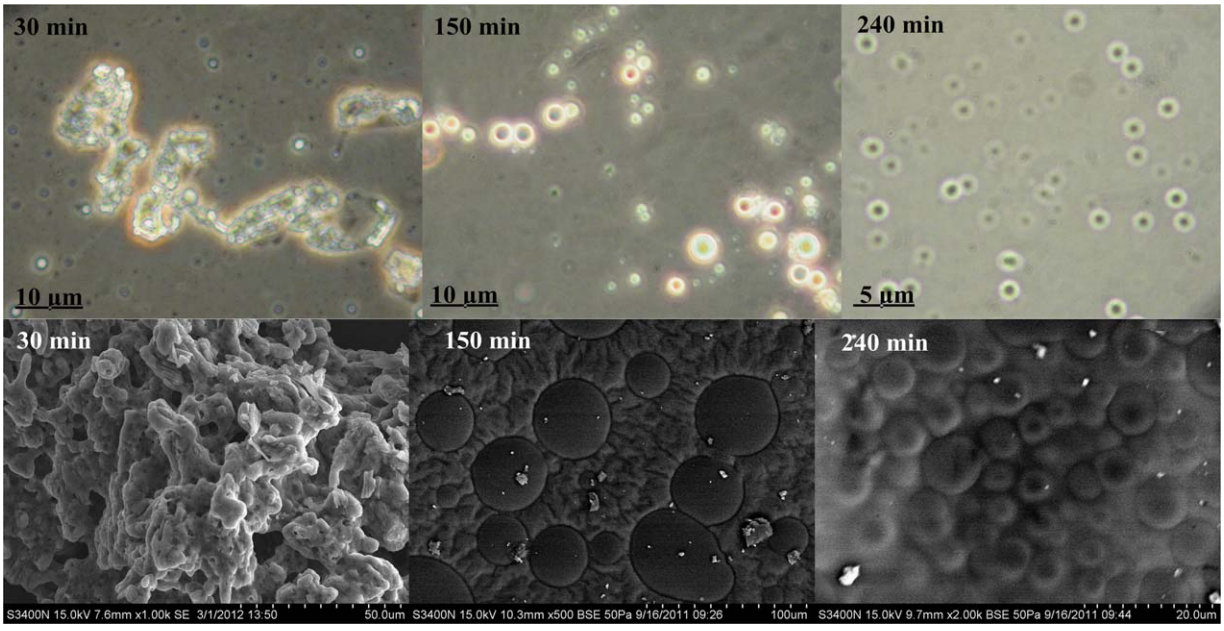

Figure 5. Images of the MEPCMs at different polymerization times by (a) phase-contrast microscopy and (b) SEM. [Color figure can be viewed in the online issue, which is available at wileyonlinelibrary.com.]

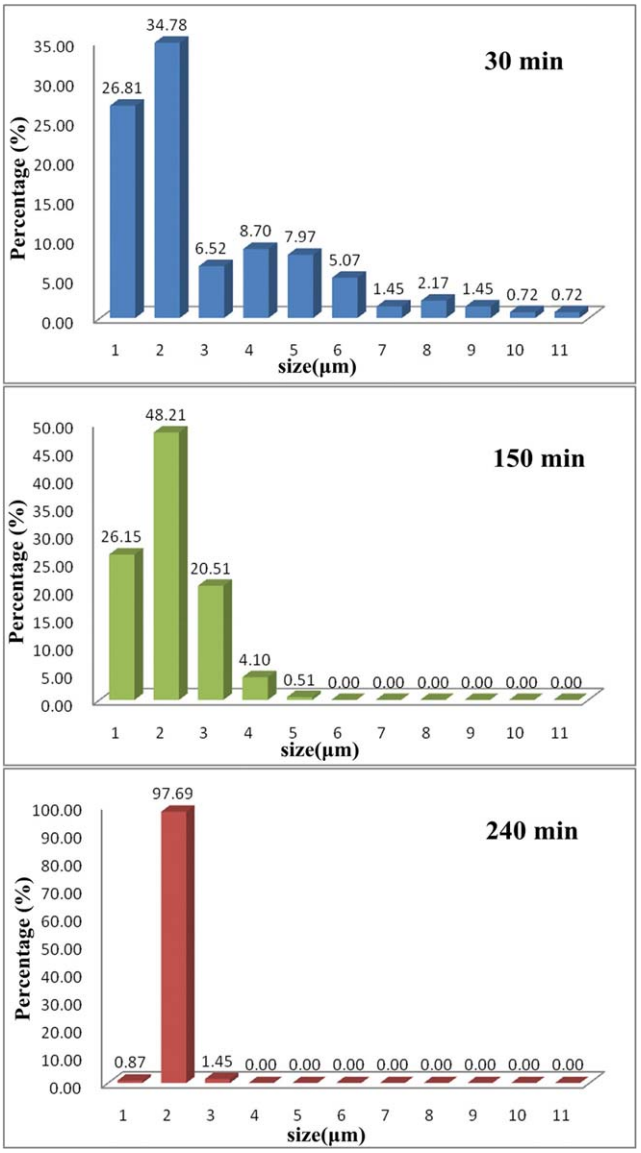

Figure 6. Diameter distribution of the MEPCMs prepared at different polymerization times. [Color figure can be viewed in the online issue, which is available at wileyonlinelibrary.com.]

$$Na_2HPO_4 \cdot 12H_2O(s) \xrightarrow{25\sim55^{\circ}C} Na_2HPO_4 \cdot 7H_2O(s) + 5H_2O(g) \quad (1)$$

In addition, it is worth noting that the two peaks appeared in the curve at 34.45 and 50.74°C in the MEPCM D_2 spectrum (Figure 3). This outcome might have occured because of the complex changes in the core material during the preparation process; this made the D_2 samples undergo phase separation; part of the core material was coated with DSP, and the rest was clad with $Na_2HPO_4{\cdot}7H_2O$. Therefore, the T_m of the two peaks of the D_2 MEPCM samples may be corresponded to pure $Na_2HPO_4{\cdot}12H_2O$ and $Na_2HPO_4{\cdot}7H_2O$, respectively.

Influence of the Type of Organic Solvents

The microencapsulation process could be achieved through the liquid phase separation of the organic phase; this requires: (1) the core material to be dispersed well in organic solvent A, (2) the shell material monomer, MMA, could be dissolved in the volatile organic solvent B and also in solvent A, and (3) organic solvent B to act as a condensed medium; this made the shell materials partially crystalline at the same time that the cross-linking monomer EA was added to the dispersed-phase organic solvent A and suspension polymerization was achieved.

The shell material PMMA was formed by the copolymerization of double bonds of MMA and the second monomer EA. The suspension polymerization occurred at 80–90°C when the functional additives were added. In this microencapsulation process, the precipitation and dispersion of the polymers relied on the volatilization of the volatile organic solvent B. Therefore, the physical and chemical properties of the volatile organic solvent and the solvent–polymer interactions had a strong impact on the formation of the MEPCMs.

In this study, different types of organic solvents (A and B) were used in the preparation of microcapsules, and DSC measurement was used to investigate the T_m and ΔH values of the MEPCMs. The corresponding DSC curves are shown as Figure 4. As shown in thsi figure, the T_m values of batches 1, 2, and 3 were about 51°C, as discussed before. Furthermore, the solubility of MMA varied with different organic solvents, and this led to the different filling rates for the core material to the total microcapsules and the formation of different phase-transition enthalpies. From this point of view, it could reach a large phase-transition enthalpy of 173.9 J/g when with acetone and carbon tetrachloride were used as the organic solvents.

Influence of the Polymerization Time

The size and morphology of the MEPCMs as influenced by the polymerization time were investigated, as shown in Figure 5. The polymerization time strongly affected the degree of completeness of the polymerization reaction. The results indicate that there would be more spherical particles if they had sufficient polymerization time. Obviously, the case of capsule formation followed the same rule as the suspension polymerization process. After BPO used as a radical initiator was added last to start this polymerization, the polymerization was complete at 80–90°C for some time. As shown in the figure, when the polymerization was complete by 30 min, the shell material formed gradually and showed an unsmooth, floc-mud-like structure. When polymerization was completed by 150 min, the shell material was further generated, and this resulted in a unsmooth block of microcapsules. This might have been because of the incomplete polymerization; the shell material was not fully formed, and this led to almost no generated single independent spherical microcapsules. However, when the polymerization was completed by 240 min, the microcapsules almost formed smooth spheres. The diameter of the microcapsules were small and evenly distributed with no agglomeration. This was due to the sufficient polymerization time; the shell material formed completely, and every microcapsule showed an independent existence state.

At the same time, as observed in Figure 6, the uniform size distribution of the MEPCMs according to the phase-contrast microscopy images remained unchanging at approximately 3.58, 2.41, and 2.12 μm, values that corresponded to times of 30, 90,

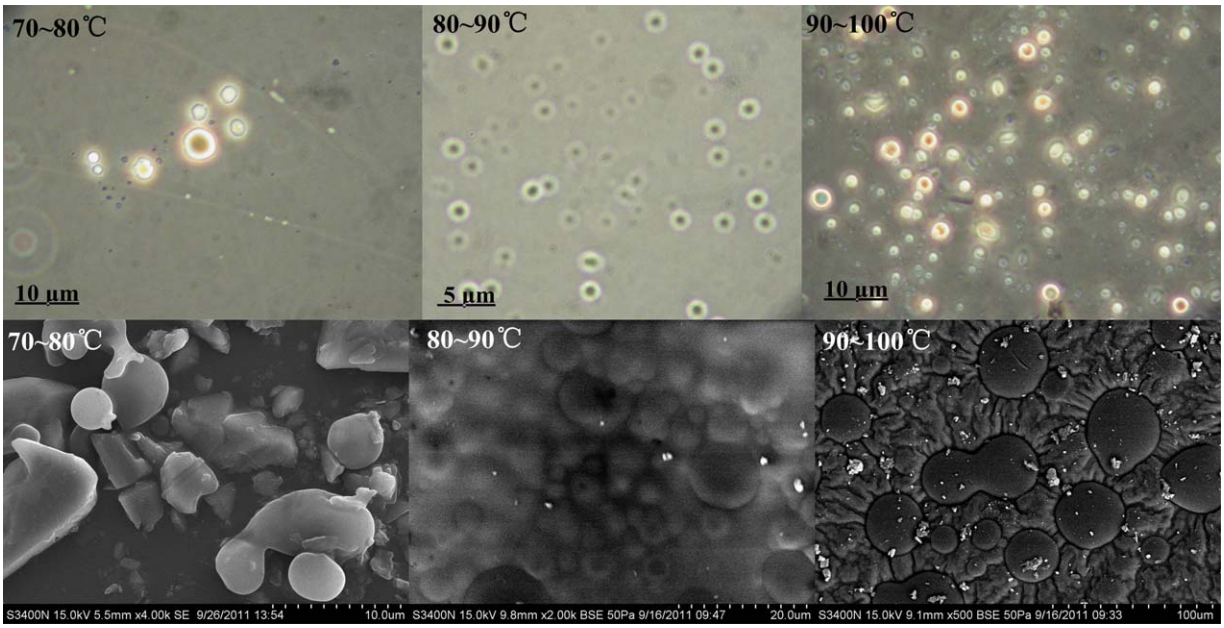

Figure 7. Images of the MEPCMs at different polymerization temperatures by (a) phase-contrast microscopy and (b) SEM [Color figure can be viewed in the online issue, which is available at wileyonlinelibrary.com.]

and 240 min, respectively. The particle size distribution was uniform in the range 1–10 μm. Because the polymerization occurred in liquid, and the water and organic phases were dispersed into small emulsion droplets fully in 5 min. The formation of the microcapsule particle size was ultimately decided by the droplet diameter. As expected, the different polymerization times have barely any effects on the size distribution, but strongly influenced the morphology of the MEPCMs in contrast.

Influence of the Polymerization Temperature

In the suspension polymerization system, the polymerization temperature had a great impact on the morphology and structure of the microcapsules.[31] The synthesis of the MEPCMs under different polymerization temperatures was investigated. Figure 7 displays the surface morphology of the microcapsules obtained by phase-contrast microscopy and SEM. When the MEPCMs was prepared for 240 min and the polymerization temperature was 70–80°C, a small amount of microcapsule formed by spherical rules. This fact indicated that the shell formed incompletely, and this led to a block of microcapsules appearing. It seemed clear that the reaction temperature had to be higher than the self-accelerating polymerization temperature of the initiator, which was established by the supplier as 80°C; otherwise, the microencapsulation was not finished. There are probably radicals below that value but not enough to complete the polymerization reaction in the case.

At the same time, when the polymerization temperature was 80–90°C, the microcapsules obtained did have a typical homogeneous spherical shape with good distribution on the mesoscopic scale. As expected, the average diameter was 2.41 μm, as obtained by the statistics of more than 100 microcapsules from the images of phase-contrast microscopy and SEM. On the other hand, when the polymerization temperature was 90–100°C, the surface morphology of the microcapsules began to agglomerate because of the shell materials reuniting with each other, and multicore microcapsules appeared. The microcapsule spheres grew larger, and the number-average diameter was 3.81 μm. This fact could be explained by the shorter half-life of BPO at higher temperatures, which led to a lower efficiency of the initiation of polymerization and resulted in a greater instability of the encapsulation process. This was reflected in an irregular particle morphology or could even be considered as a case of dead-end polymerization, as described by Odian.[22]

Likewise, as shown in Figure 8, slightly above the activation temperature of the initiator (80–90°C), the uniform size distribution of MEPCMs in the range 1–10 μm and the average size according to the phase-contrast microscopy images remained unchanging (ca. 2.41 μm) because the formation of the microcapsule particle size was ultimately decided by the droplet diameter, not the polymerization temperature. Hence, the size distribution was more influenced by the type of stirring, the addition of surfactants, or the hydrophilic nature of the polymer than by the temperature. Our system revealed the typical behavior of a suspension polymerization, where the reaction temperature barely affected the time needed to reach the identity point.

CONCLUSIONS

Novel MEPCMs of $Na_2HPO_4{\cdot}12H_2O$–PMMA were successfully prepared through a solvent evaporation technique. On the basis of the analysis of influence factors, the reaction temperature had very little effect on the particle size distribution but did have an effect on the surface morphology. A synthesis temperature of 80–90°C, a reaction time of about 240 min, and a

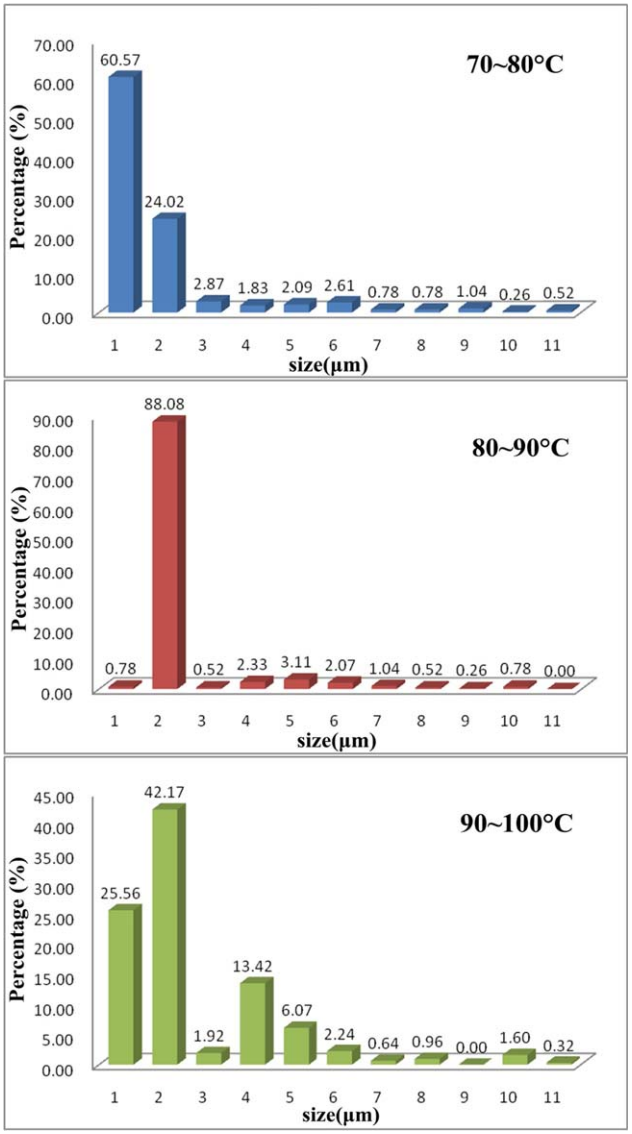

Figure 8. Diameter distribution of the MEPCMs prepared at different polymerization temperatures. [Color figure can be viewed in the online issue, which is available at wileyonlinelibrary.com.]

higher stirring rate (900 rpm) were the most admirable parameters for the microencapsulation process. In addition, upon the investigation of the influence of organic solvent types on the thermal properties of the MEPCMs, we noted that a T_m of about 51°C was a significant increase relative to that of pristine DSP (ca. 17°C), whereas their ΔH values decreased. This was mainly due to the interfacial interactions between the core and shell materials, and the core material complex may have changed so that $Na_2HPO_4{\cdot}7H_2O$ was confined in the microcapsules during the preparation process; this makes it suitable for different applications, especially in the thermal field.

ACKNOWLEDGMENTS

The authors acknowledge financial support from the National Natural Science Foundation of China (contract grant number 51006024); the Scientific and Technological Project of Guangdong Province (contract grant number 2010B060900003); the Special Funding of Combination of Production, Teaching and Research of Guangdong Provincial and the National Ministry of Education (contract grant number 2011B090400446); and the Special Funding of Colleges and Universities Discipline Construction of Guangdong Province (contract grant number 2012KJCX0041).

REFERENCES

1. Zhang, Y. L.; Rao, Z. H.; Wang, S. F.; Zhang, Z.; Li, X. P. *Energy Convers. Manage.* **2012**, *59*, 33.
2. Su, J. F.; Wang, X. Y.; Huang, Z.; Zhao, Y. H.; Yuan, X. Y. *Colloid Polym. Sci.* **2011**, *289*, 1535.
3. Yu, F.; Chen, Z. H.; Zeng, X. R. *Colloid Polym. Sci.* **2009**, *287*, 549.
4. Do, C. V.; Nguyen, T. T. T.; Park, J. S. *Solar Energy Mater. Solar Cells* **2012**, *104*, 131.
5. Basal, G.; Deveci, S. S.; Yalcin, D.; Bayraktar, O. *J. Appl. Polym. Sci.* **2011**, *121*, 1885.
6. Alkan, C.; Ensari, Ö. F.; Kahraman, D. *J. Appl. Polym. Sci.* **2012**, *126*, 631.
7. Luz, S. S.; Juan, F. R.; Carmona, M.; Romero, A.; Sánchez, P. *J. Appl. Polym. Sci.* **2011**, *120*, 291.
8. Huang, J.; Wang, T. Y.; Wang, C. H.; Rao, Z. H. *Mater. Res. Innovations* **2011**, *15*, 422.
9. Rao, Z. H.; Wang, S. F.; Zhang, Y. L. *Phase Transitions* **2012**, *85*, 400.
10. Su, J. F.; Wang, S. B.; Zhang, Y. Y.; Huang, Z. *Colloid Polym. Sci.* **2011**, *289*, 111.
11. Wang, Y.; Shi, H.; Xia, T. D.; Zhang, T.; Feng, H. X. *Mater. Chem. Phys.* **2012**, *135*, 181.
12. Li, J. L.; Xue, P.; Ding, W. Y.; Han, J. M. *Solar Energy Mater. Solar Cells.* **2009**, *93*, 1761.
13. Chen, C. M.; Chen, Z. H.; Zeng, X. R.; Fang, X. M.; Zhang, Z. G. *Colloid Polym. Sci.* **2012**, *290*, 307.
14. Luz, S. S.; Juan, F. R.; Romero, A.; Sánchez, P. *J. Appl. Polym. Sci.* **2012**, *124*, 4809.
15. Chang, C. C.; Tsai, Y. L.; Chiu, J. J.; Chen, H. *J. Appl. Polym. Sci.* **2009**, *112*, 1850.
16. Saadat, Y.; Hosseinzadeh, S.; Eslami, H., Afshar-Taromi, F. *Colloid Polym. Sci.* **2012**, *290*, 1099.
17. Zhang, J.; Wang, S. S.; Zhang, S. D.; Tao, Q. H.; Pan, L.; Wang, Z. Y.; Zhang, Z. P. *J. Phys. Chem. C.* **2011**, 115, 20061.
18. Salaün, F.; Devaux, E.; Bourbigot, S.; Rumeau, P. *Carbohydr. Polym.* **2010**, *79*, 964.
19. Luz, S. S.; Rodríguez, J. F.; Sánchez, P. *Colloids Surf. A* **2011**, *390*, 62.
20. Niu, X. W.; Sun, Y. M.; Ding, S. N.; Chen, C. C.; Song, B.; Xu, H.-B.; Qi, Z.-J.; Qi, Q. Q. *J. Appl. Polym. Sci.* **2012**, *124*, 248.
21. Lu, S. F.; Xing, J. W.; Zhang, Z. H.; Jia, G. P. *J. Appl. Polym. Sci.* **2011**, *121*, 3377.

22. Luz, S. S.; Sánchez, P.; Carmona, M.; Lucas, A. D.; Rodríguez, J. F. *Colloid Polym. Sci.* **2008**, *286*, 1019.

23. Su, J. F.; Wang, X. Y.; Dong, H. *Mater. Lett.* **2012**, *84*, 158.

24. Chen, L.; Zhang, L. Q.; Tang, R. F.; Lu, Y. L. *J. Appl. Polym. Sci.* **2012**, *124*, 689.

25. Ma, S. D.; Song, G. L.; Li, W.; Fan, P. F.; Tang, G. Y. *Solar Energy Mater. Solar Cells.* **2010**, *94*, 1643.

26. Song, J.; Chen, L.; Li, X. J. Microencapsulation Technology and Applications; Chemical Industry Press: China, **2001**; p 1.

27. Alcoutlabi, M.; McKenna, G. B. *J. Phys.: Condens. Matter* **2005**, *17*, R461.

28. Pan, L.; Tao, Q. H.; Zhang, S. D.; Wang, S. S.; Zhang, J.; Wang, S. H.; Wang, Z. Y.; Zhang, Z. P. *Solar Energy Mater. Solar Cells* **2012**, *98*, 66.

29. Yan, Y.; Lin, X. H.; Zhang, H. P. *High School Chem. Eng. School Newspaper* **2011**, *6*(25), 1068.

30. Ghule, A.; Bhongale, C.; Chang, H. *Spectrochim. Acta A* **2003**, *59*, 1529.

31. Li, W.; Song, G. L.; Tang, G. Y.; Chu, X. D.; Ma, S.; Liu, C. F. *Energy.* **2011**, *36*, 785.